

Development of a Novel Condensing Porous Heat Exchanger (CPHE) with integrated Porous Burner (PB)

Maka P, Kaewpradap A and Jugjai S*

Combustion and Engine Research Laboratory (CERL),
Department of mechanical Engineering, Faculty of Engineering, King Mongkut's University of Technology Thonburi,
126 Prachauthit Road (Suksawad 48) Bangmod, Thung Kharu District, Bangkok 10140

*Corresponding Author: E-mail: sumrueng.jug@kmutt.ac.th, Tel: (662) 4709128, Fax: (662) 4709111.

Abstract

Porous medium is a special material because it can promote heat transfer, heat recirculation, and high radiative property. By these advantages the porous medium can be both a combustor and a heat exchanger. In this study a condensing porous heat exchangers (CPHE) with integrated porous burner (PB) is investigated to clarify heat transfer performance and emission characteristics. The PB is operated as non-premixed combustion mode. Liquefied petroleum gas and air are separately supplied into the PB. Annular flow of air is covering the axial flow of fuel when the mixing chamber is completely closed; the diffusion flame mode is established. The CPHE consists of three parts, i.e. an upper jacket, a lower jacket and a tube bank. The tube bank that was staggered of six rows and cross flow was embedded within porous medium. Alumina balls (Al_2O_3) of size 10 mm and 15 mm were packed in PB and CPHE, respectively. The effect of the firing rate (FR) on the temperature profiles, total thermal efficiency, heat transfer performance, effectiveness, heat transfer coefficient (h_o), and overall heat transfer coefficient (U) was investigated. CO and NO_x emissions were measured and compared with the combustion within a non-porous heat exchanger (N-PHE). The results show that the combustion zone can be located and stabilized within the PB. When FR increases combustion zone moves downstream. Similarly staged combustion, the reaction zone extends into the CPHE, promoting heat transfer performance and yielding high total thermal efficiency. Heat transfer into tube banks was significantly higher than that transfer to upper and lower jackets due to the enhancements of the heat transfer within porous medium. CO and NO_x emissions were under standard of Thailand. Moreover, the heat transfer coefficient (h_o), the overall heat transfer coefficient (U) and effectiveness (ε) of CPHE are higher than those of N-PHE, and the same results go for every other factors. The values of h_o and U are 4 and 5.76 time higher than N-PHE, respectively, with effectiveness is as high as 0.97. Moreover, the condensation of exhaust gases was achieved. This confirms that the porous medium successfully promotes heat transfer.

Keywords: porous medium, porous burner, condensing porous heat exchanger, effectiveness.

AEC007

1. Introduction

Combustion of premixed and non-premixed gases in porous medium combustor has been continuously studied and developed by Combustion and Engines Research Laboratory (CERL) of KMUTT [1-2]. The porous medium provides heat recirculation from the hot exhaust gas to the upstream mixture via heat conduction and radiation in the porous medium. Due to its advantages such as super adiabatic combustion temperature, high radiant intensity and low pollutant emissions, these extend flammability and stability limits, compared with the conventional combustion. And hence, the porous medium can be both a combustor and a heat exchanger.

Mohammad [3] numerically studied the convective heat transfer of flow past embedded staggered tube bank within porous medium. The results demonstrated that the Nusselt number (Nu_D) of embedded tube bank in porous is higher than without porous. The Nu_D of the first row is lower than another row and it became turbulent flow since the second row and beyond. Jugjai and Pookertsin [4] conducted correlation of the total

thermal resistance with the experimental study on the porous combustor-heater (PCH), which is a combustion heat transfer device involving relatively cold heat exchanger surface embedded directly in the porous medium, in which gaseous fuel is burned. Moreover, [4] adapted correlation of Nu_D from [3] for calculate of flow past embedded staggered tube bank within porous medium.

Because the PB provides several advantages compared to the conventional burner. Thus, in this study a condensing porous heat exchangers (CPHE) with integrated porous burner (PB) is investigated to clarify heat transfer performance and emission characteristics. The CPHE was designed by using correlation of the total thermal resistance in porous medium. In addition, the effect of the firing rate (FR) on the temperature profiles, total thermal efficiency, heat transfer performance, effectiveness, heat transfer coefficient (h_o), overall heat transfer coefficient (U) and pollution emissions of CO and NO_x are investigated and compared with the combustion within a N-PHE.

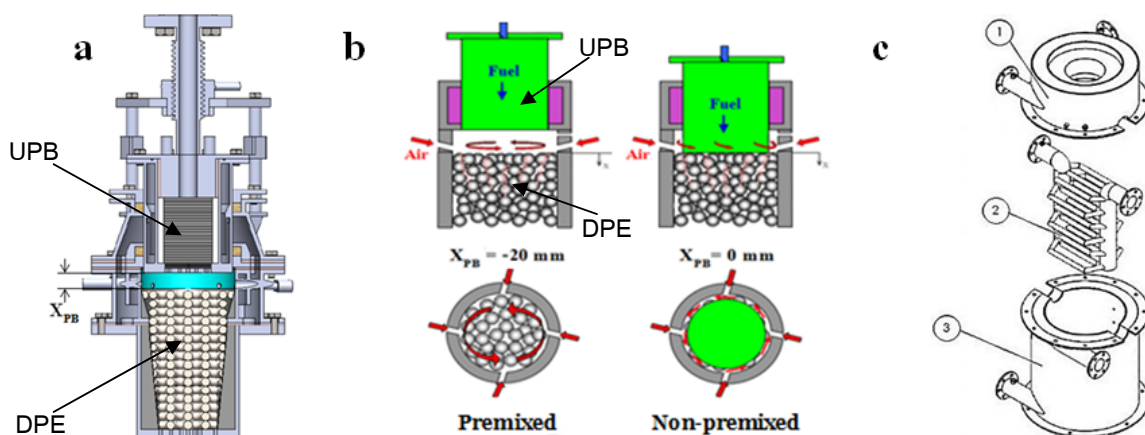


Fig. 1 a. the distance of mixing chamber in the porous burner (PB), b. The combustion mode, c. The schematic structure of CPHE.

Table. 1 Nomenclatures

Symbols	Subscripts	Greek Symbols			
A	heat transfer area of the tube (m^2)	c	cold fluid	ε	effectiveness (-)
FR	firing rate (kW)	exp	calculated from the experiment	η	thermal efficiency
C	heat capacity rate ($W/^\circ K$)	h	hot fluid		
C_p	specific heat ($J/kg\text{-}^\circ K$)	i	inlet (for T) or inside tube (for h or r)		
HHV	high heating value (kJ/kg)	lm	log mean temperature difference		
h	heat transfer coefficient ($W/m^2\text{-}^\circ K$)	low	lower water jacket		
k	thermal conductivity ($W/m\text{-}K$)	o	outlet (for T) or outside tube (for h or r)		
\dot{m}	mass flow rate (kg/s)	rad	radiation		
Q	heat transfer rate (kW)	s	surface		
r	radius (m)	up	upper water jacket		
T	temperature ($^\circ K$)				
U	overall heat transfer coefficient ($W/m^2\text{-}^\circ K$)				

2. Experiments

2.1 Experimental apparatus

The PB consists of two parts, i.e., an upstream porous burner (UPB) and a downstream porous emitter (DPE). The PB is movable in a telescopic manner and provides a free space between UPB and DPE that is called a mixing chamber. Fig. 1a shows the distance of mixing chamber which is defined as X_{PB} . The combustion mode can be controlled by the telescopic action of the UPB.

At $X_{PB} = -20$ mm is fully opened mixing chamber while the $X_{PB} = 0$ mm is completely closed mixing chamber. Hence, premixed and non-premixed combustion mode is established, respectively, as express in Fig. 1b. More detailed of the PB can be found in the previous study [2]. The schematic structure of the CPHE is shown in Fig. 1c. The CPHE was made from SUS 304 stainless steel. It consists of three parts, i.e.: upper water jacket, lower water jacket and tube bank. The upper and lower water jackets were specially designed to minimize radiative heat loss from combustion product. The tube bank consists of 21 tubes that were staggered of six rows and cross flow. It was embedded within spherical alumina pellets to serve as a thermal load. Each tube was 12.6 mm in diameter and 171 mm in length. The pitch distance of tube arrangement is chosen from the previous work of Jugjai and Pookertsin [4] which allow the combustion zone to be located and stabilized within tube bank.

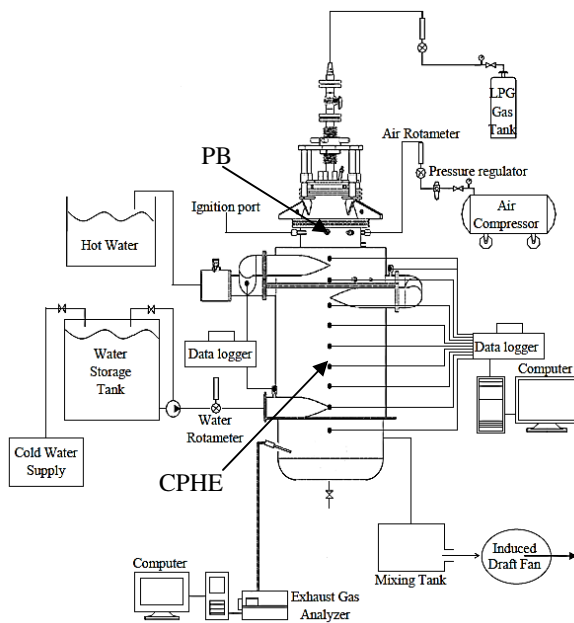


Fig. 2 Schematic diagram of the experimental apparatus.

2.2. Experimental setup

Fig. 2 shows the schematic diagram of the experimental apparatus. The apparatus consists of three main parts: fuel, air and water supply system, data acquisition system and CPHE. The PB was installed above the CPHE. The air was

AEC007

supplied by an air compressor, while the fuel was supplied from cylinders of compressed liquefied petroleum gas (LPG 60% propane, 40% butane; 49,840 kJ/kg). Gas and air flow rates were measured by calibrated rotameters.

Temperature of combustion gas were measured along the centerline of CPHE by using B-type thermocouple (i.e., T6-T7 in the burner) and N-type thermocouple (i.e., T8-T15 in the heat exchanger) as show in Fig. 3a. In addition, the inlet and outlet water temperatures for lower jacket (T1-T2), tube bank (T2-T3), upper jacket (T4-T5), and flow path of water were also measured (by N-type thermocouple) and was show in Fig. 3b. Their signals are digitized by a general-purpose DT 600 Data logger, and then are transmitted to a personal computer.

A pump of water supply system was used to ensure that the water is fully flowing through the cross-sectional area of heat exchanger which can see water flow through transparent tube. The water flow rate (\dot{m}_w) was measured by calibrated rotameter. In the experiments, the water flow rate was kept constant at 9.5 kg/min.

The Messtechnik Eheim model Visit01L which is a portable emission analyzer designed especially for quasi-continuous measurement was used to analyze the emission of the dry combustion products at the exit of the CPHE. The measuring range is 0–4000 ppm for NO_x and 0–10,000 ppm for CO with the accuracy of about ±5 ppm and the resolution of 1 ppm for both NO_x and CO. All measured emissions in the experiment are corrected to 0% excess oxygen and dry-basis.

2.3. Procedure

LPG and air are separately supplied into the

Table. 2 Operating condition.

Quantity	value
Alumina pellets diameter, d_p	15×10^{-3} m
Equivalence ratio, ϕ	0.46
Firing rate, CL	5-20 kW
High heating value of LPG	49,840 kJ/kg
Inlet temperature of water, $T_{w,in}$	305 K
Inside surface area per one tube, $A_i = \pi D_m L$	0.0048 m^2
Number of tubes of tube bank	21
Outside surface area per one tube, $A_o = \pi D_{out} L$	0.0068 m^2
Porosity, ϕ	0.41
Total water mass flow rate at tube bank, $\dot{m}_{w,tb}$	9.5 kg/min
Total heat transfer surface area, $A_b = 21 \cdot A_o$	0.143 m^2
Tube inside diameter, D_m	9×10^{-3} m
Tube outside diameter, D_{out}	12.6×10^{-3} m
Water tube thermal conductivity, k_{ss}	13.4 W/m-K

PB. Combustion was started with premixed flame mode ($X_{PB} = -20$). Premixed gases with near stoichiometry condition were supplied into the combustion chamber at firing rate (FR) of 5 kW. Ignition start by using an auxiliary pilot flame injected through an ignition port. Once ignition is accomplished, the auxiliary flame was removed and the combustion was switched into diffusion flame mode ($X_{PB} = 0$). During the preheating period, the cooling water was supplied to the CPHE to prevent overheating. Then, gradually adjusted the FR , ϕ , and \dot{m}_w to obtain the desired operating condition. As soon as a steady state condition was reached, the data were recorded. All numerical values of operating conditions appearing in the experiment are summarized in Table. 2.

3. Method of data analysis

In this study, heat transfer of the CPHE is calculated by the heat transfer rate from heat loss of hot gas transferring to the water (Q_h) and the heat gained by the water (Q_c). These can be expressed by Eqs. (1) and (2).

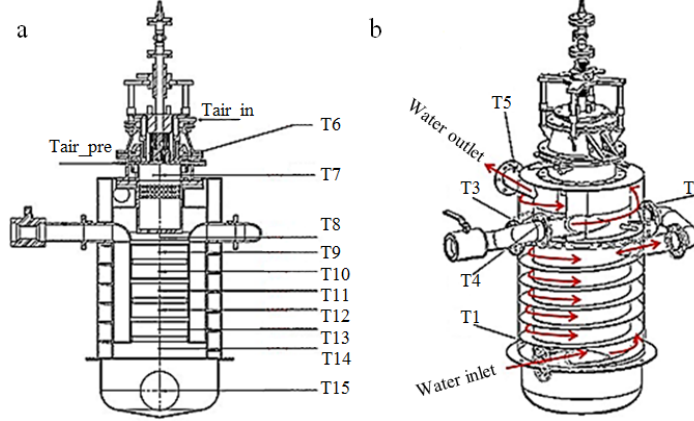


Fig. 3 Temperature measurement in the CPHE. (a) Gas, (b) Water.

$$Q_h = \dot{m}_h c_{p,h} (T_{h,i} - T_{h,o}) \quad (1)$$

$$Q_c = \dot{m}_c c_{p,c} (T_{c,i} - T_{c,o}) \quad (2)$$

where \dot{m} is the water mass flow rate and c_p is the specific heat of hot and cold fluid with subscript h and c , respectively. The heat transfer performance in this study can be explained by total thermal efficiency as show in Eq. (3).

$$\eta_{total} = \eta_{up\ jacket} + \eta_{tube\ bank} + \eta_{low\ jacket} \quad (3)$$

where η_{total} is defined as a summation of the thermal efficiency of the CPHE. The thermal efficiency is the ratio of the rate of heat absorbed by the water flowing in each part of the CPHE to the firing rate (FR) which can be obtained from high heating value of fuel (the water condensation from exhaust gases) as show in Eq. (4).

$$FR = \dot{m}_{fuel} \times HHV \quad (4)$$

where \dot{m}_{fuel} is the mass flow rate of fuel. To investigate the overall heat transfer coefficient (U) of the tube bank form experiment, the logarithmic mean temperature difference (ΔT_{lm}) and the

heat transfer rate to tube was calculate by Eqs. (5), (6), (7), respectively.

$$U_{exp, tube\ bank} = \frac{Q_{exp, tube\ bank}}{\Delta T_{lm} A_s} \quad (5)$$

where A_s is the heat transfer area.

$$\Delta T_{lm} = \frac{\Delta T_2 - \Delta T_1}{\ln(\Delta T_2 / \Delta T_1)} \quad (6)$$

where $\Delta T_1 = T_{h,8} - T_{c,3}$ and $\Delta T_2 = T_{h,14} - T_{c,2}$

$$Q_{exp, tube\ bank} = \dot{m}_h c_{p,h} (T_{h,8} - T_{h,14}) - [\dot{m}_c c_{p,c} (T_{c,2} - T_{c,1})]_{low\ jacket} \quad (7)$$

In this experiment, the convective heat transfer coefficient (h_o) is the important variable which controls heat transfer rate to tube bank. Previously, the work of Jugjai and Pookertsin [4] proposed the total thermal resistance of the porous combustor-heater (PCH), which calculated h_o for flow past embedded staggered tube bank within porous medium and gaseous fuel was burned in the porous medium (the configuration is similar to this work) as expressed by Eq. (8).

AEC007

$$h_{o,exp,tubebank} = \frac{1}{\left[\frac{1}{U_{exp,tubebank}} \frac{r_o \ln(r_o/r_i)}{k_{tube}} - \frac{r_o}{h_i r_i} \right] - \frac{k_{eff(s-g)}}{r_o \ln(2z/r_o)} - \frac{k_{rad}}{r_o \ln(2z/r_o)}} \quad (8)$$

where $k_{eff(s-g)}$ is an effective thermal conductivity of packed bed and k_{rad} is the radiative thermal conductivity of packed bed that expressed by [4]. The effectiveness is defined as the fraction of the actual heat transfer rate to the maximum possible heat transfer rate that can be given in Eq. (9).

$$\varepsilon = \frac{Q_{actual}}{Q_{max}} = \frac{C_h (T_{h,i} - T_{h,o})}{C_{min} (T_{h,i} - T_{c,i})} \quad (9)$$

where $C_h = \dot{m}_h c_{p,h}$ is heat capacity rate of hot fluid and C_{min} is minimum heat capacity rate of fluid (hot fluid).

4. Results and discussion

In this study thermal performance of CPHE was experimentally investigated. The experimental results are performed at different firing rate (i.e., $FR = 5 - 20$ kW) with equivalence ratio of 0.46 (for CPHE) and 0.61 (for N-PHE) that is a good condition of emission pollution of each type. By using the experimental data, effectiveness, heat transfer, total thermal efficiency and coefficient of heat transfer were calculated. Fig. 4 shows the effect of CPHE and N-PHE on the temperature distributions along the centerline under different firing rate. It is clearly seen that the maximum combustion temperatures increases with FR , since the thermal input is proportional to it. Although, the combustion temperature in PB of CPHE is higher than that of N-PHE, the highlight of this figure is marked decrease in temperature in CPHE. Moreover, the

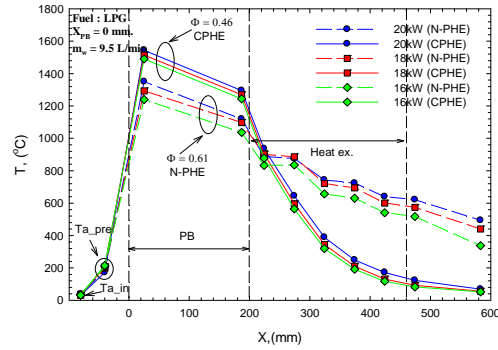


Fig. 4 Effect of CPHE and N-PHE on the temperature distributions along the centerline of CPHE.

condensation of exhaust gases was achieved. These results indicate that porous medium within heat exchanger is successfully promoting the heat transfer performance.

Fig. 5 shows variations of effectiveness and heat transfer rate (lower jacket and tube bank) versus firing rate between CPHE and N-PHE. The effectiveness is an indicator of the heat exchanger performance, and it is used as a design factor to find the maximum usage of thermal energy output. The effectiveness gradually decreased with increasing of the firing rate, and hence, it results to higher heat loss of burner. The effectiveness of the CPHE is higher than that of the N-PHE. In the experimental

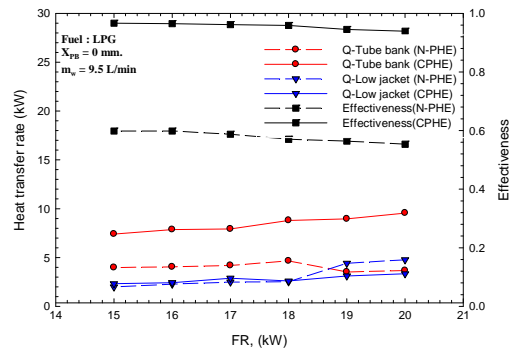


Fig. 5 Effect of FR on effectiveness and heat transfer rate.

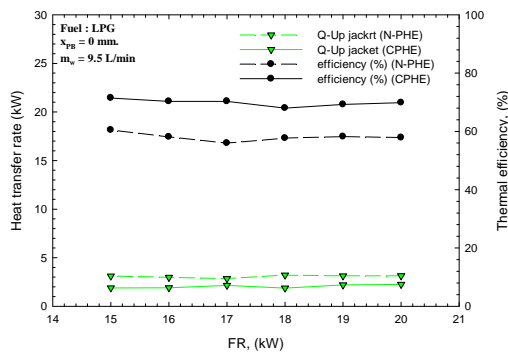


Fig. 6 Effect of FR on total thermal efficiency and heat transfer rate.

range, the highest effectiveness value was approximately 0.97 at equivalence ratio of 0.46 for the CPHE. Furthermore, heat transfer rate of the CPHE transferring to tube bank is the highest, and it is higher than that of the N-PHE, because high flame temperature can take place close to tube bank in the small voids between the particles. Hence, it enhances the radiant heat transfer from the solid particles to tube bank. In addition, gas flow across the tube bank is well mixed and the turbulent flow was produced by the solid particles in the bed. The increase in flow velocity results to the thinness of thermal boundary layer around tube surface. In contrast, heat transfer rate of both heat exchanger to upper and lower jacket are similar values.

Fig. 6 shows the total thermal efficiency and heat transfer rate (of the upper jacket) with variations of firing rate between CPHE and N-PHE. The increase in total thermal efficiency of CPHE is expected because the heat transfer rate to tube bank is increased as shown in Fig. 5.

Fig. 7 shows the CO emissions of CPHE and N-PHE. The CO emission of the CPHE is lower than that of the N-PHE and it is lower than the limits of the standard of American (ANSI Z21.1)

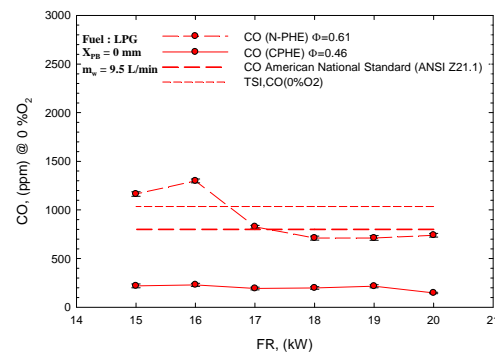


Fig. 7 The CO emissions of CPHE and N-PHE. and Thailand. It can be described by the same result of heat transfer rate into tube bank of the CPHE, which reduces CO formation from flame quenching effect.

Fig. 8 shows NO_x emissions of the CPHE and the N-PHE. As expected, NO_x emissions of the two heat exchangers are steadily constant with increasing FR , because the combustion zone can be located and stabilized within the PB. It has ability to reduce NO_x formation by similarly staged combustion technic. Thus, low emissions of NO_x are yielded and they are lying under standard of Thailand. Increasing of CO emission at low FR of N-PHE because a poor mixing of the combustible mixture in the PB which accord with flow velocity of air.

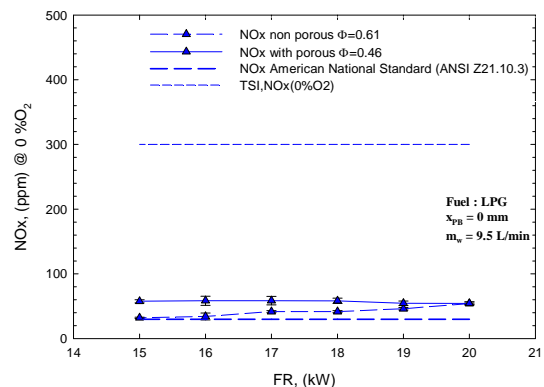


Fig. 8 The NO_x emission of CPHE and N-PHE.

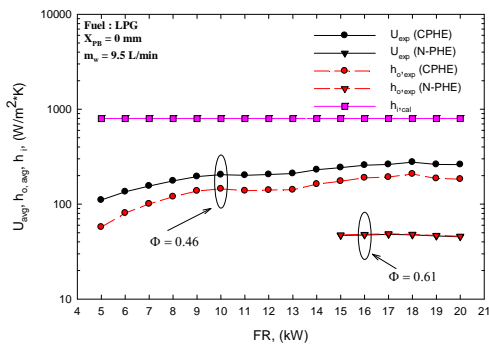


Fig. 9 The heat transfer coefficient of CPHE and N-PHE.

Fig. 9 shows the heat transfer coefficient of the CPHE and the N-PHE. Since the mass flow rate of water was kept constant, thus, the heat transfer coefficients in tube bank of the two heat exchangers are equal. However, the U and h_o of the CPHE is higher than that of the N-PHE, because porous medium in heat exchanger promotes heat transfer coefficient by the increase in flow velocity when the flow passing small void of solid particles and created turbulent flow. In addition, the reaction zone that extends into the CPHE can be occurred even though it is close to tube bank. Hence, it enhances conduction and radiation heat transfer to tube bank. The U and h_o was calculated from experimental data by using Eqs. (7) - (8).

5. Conclusions

The main goal of this research is to acquire the knowledge for the development of the CPHE technology in terms of the increase of energy efficiency and decrease of the pollution emissions of CO and NO_x. The main results are summarized as follows:

5.1 Porous medium within tube bank heat exchanger can promotes U and h_o resulting in an

increasing of heat transfer into tube bank. The high flame temperature can be taken place close to tube bank, which enhances the radiant heat transfer.

5.2 The CPHE yields higher effectiveness and total thermal efficiency than those of the N-PHE system with a significantly lower CO emission, but, with almost the same value of NO_x. The current experimental work demonstrates that the CPHE with the tube bank embedded is an innovative and effective method for fluid heating devices.

6. References

- [1] Jugjai, S. and Toklib, P. (2010). Porous Burner with Non-premixed and Premixed Combustion, paper presented in *The 24th Conference of Mechanical Engineering Network of Thailand*, Ubon Ratchathani, Thailand.
- [2] Jugjai, S. and Homrarueng, A. (2014). An Experimental Study on Combustion Performance of Flexible Porous Medium Burner (FPMB), paper presented in *The 5th TSME International Conference on Mechanical Engineering*, Chiang mai, Thailand.
- [3] Mohammad, L. (2008). Numerical Analysis of Wooden Porous Media Effects on Heat Transfer from Staggered Tube Bundle, *Journal of Heat transfer*, Vol. 130(1), pp. 014501-1 - 014501-6.
- [4] Jugjai, S. and Pookertsin, P. (2011). The study of combustion and heat transfer performance of porous combustor-heater with in-bed heat extraction, paper presented in *The 2nd TSME International Conference on Mechanical Engineering*, Krabi, Thailand.